

Joint Out-of-Distribution Filtering and Data Discovery Active Learning

Sebastian Schmidt^{1,2} Leonard Schenk^{3,†} Leo Schwinn¹ Stephan Günemann¹
¹ Technical University of Munich, School of Computation, Information and Technology
² BMW Group ³ SPRIND

Abstract

*As the data demand for deep learning models increases, active learning (AL) becomes essential to strategically select samples for labeling, which maximizes data efficiency and reduces training costs. Real-world scenarios necessitate the consideration of incomplete data knowledge within AL. Prior works address handling out-of-distribution (OOD) data, while another research direction has focused on category discovery. However, a combined analysis of real-world considerations combining AL with out-of-distribution data and category discovery remains unexplored. To address this gap, we propose **Joint Out-of-distribution filtering and data Discovery Active learning (Joda)**¹, to uniquely address both challenges simultaneously by filtering out OOD data before selecting candidates for labeling. In contrast to previous methods, we deeply entangle the training procedure with filter and selection to construct a common feature space that aligns known and novel categories while separating OOD samples. Unlike previous works, Joda is highly efficient and completely omits auxiliary models and training access to the unlabeled pool for filtering or selection. In extensive experiments on **18** configurations and **3** metrics, Joda consistently achieves the highest accuracy with the best class discovery to OOD filtering balance compared to state-of-the-art competitor approaches.*

1. Introduction

Deep learning models, particularly in computer vision, depend on extensive labeled datasets, which entails considerable annotation costs. Active learning (AL) offers a systematic approach to reduce annotation costs by selecting only the most informative samples for labeling. AL methodology involves a cyclic process to select previously unlabeled samples utilizing auxiliary models or properties like uncertainty or diversity.

In the classic closed set AL [53], an unlabeled pool or data stream is defined as *pure*, containing only in-distribution (InD) data that is of the same underlying distribution as the training data. Recent works [11, 39, 40, 64] propose *open-set AL* to question the real-world applicability of this assumption and consider out-of-distribution (OOD) data in the unlabeled pool. In real-world applications, data is noisy and originates from different distributions. This necessitates detecting and filtering out OOD data before selecting samples for labeling. Furthermore, dynamic and open environments contain novel objects that are absent in the training data but relevant to the task. Discovering these new InD categories is addressed by the field of category discovery [56], where incomplete knowledge about the InD data is assumed.

While existing research tends to address only one of these challenges at a time, both phenomena are likely to arise concurrently in open- or real-world applications, such as mobile robotics, environmental sensing, or autonomous driving, given the limited prior knowledge of a narrow initial dataset. Conversely, extensive data collection in real-world scenarios will inevitably lead to encounters with OOD data and novel object categories. Considering the data collection by an advanced driver assistance system of cars, in the endeavor to collect data for fully autonomous driving, unknown participants like a carriage reflect novel categories, while scenarios outside of the domain like off-road, private properties, or gravel roads pose OOD data. Especially, for autonomous driving safe operation is required [50]. Besides the limited open-world assumptions, existing works [11, 40, 44, 64] require additional models and data access to the unlabeled pool, a challenging requirement given incomplete knowledge of its data.

Our work proposes a novel approach to jointly manage impure data assumptions of open-set scenarios **and** incomplete prior knowledge assumptions of category discovery **without** using additional models or unlabeled data. We provide the following **contributions**:

- We introduce **Open-Set Discovery Active Learning (OSDAL)**, a novel scenario that jointly describes the

[†] Work done while being with TUM and BMW.

Corresponding author sebastian95.schmidt@tum.de

¹Project Page: <https://www.cs.cit.tum.de/daml/joda/>

impurity of the unlabeled data pool with the incomplete knowledge of the relevant classes (illustrated in Fig. 1).

- We propose **Joint Out-of-distribution filtering** and data **Discovery Active Learning (Joda)** as the first approach being able to separate OOD from novel classes that addresses these scenarios. Contrasting to existing works in open-set AL [11, 39, 40, 44, 64], Joda *eliminates* the need for auxiliary models and data access.
- We conduct extensive experiments on **15** settings to evaluate current AL methods and open-set AL methods. To the best of our knowledge, this is currently the largest benchmark in open-set AL. Joda confirms its effectiveness by consistently achieving the highest accuracy despite the considerably reduced complexity.

2. Related Work

Active Learning: Generally, AL focuses on strategically selecting samples for labeling to preserve high model performance while reducing the number of required annotations in stream-based or pool-based scenarios [53, 68]. Besides the classic scenarios, Schmidt and Günnemann [46] and Schmidt et al. [49] evaluated further scenarios featuring dynamic pools or batch streams. Furthermore, the various methods employed for AL are categorized into uncertainty-based, diversity-based, or model-based.

Uncertainty-based methods like ensembles [3, 30] or Monte Carlo Dropout, which leverage multiple forward passes [17, 27] select samples based on an estimated uncertainty value. Their individual sample evaluation favors them for various applications like 2D and 3D object detection [14, 19, 41, 47], semantic segmentation [24] or graphs [15]. Diversity-based approaches aim to fully cover all regions of the dataset space [52, 65]. Badge [2] combines diversity with uncertainty by gradients calculated utilizing the network’s predictions as pseudo-labels. Subsequent research follows the idea of combining uncertainty and diversity for more complex tasks like 3D object detection [37, 61]. Lastly, model-based methods employ an auxiliary model to either predict a proxy score for the sample informativeness or select samples directly. The methodology includes predicted loss values [66], encoder decoder-based approaches [26, 54, 69] or meta-models like graph neural networks [5] as well as teacher-student approaches [20, 43]. In this work, we go beyond the standard methodology used in AL and introduce aspects of OOD detection in our Joda algorithm.

Out-of-Distribution Detection: The term OOD detection is a generic term frequently used to encompass a range of related concepts, including anomaly detection, novelty detection, and open-set recognition (OSR) [45, 62]. In a common understanding of OOD detection, a sample must be categorized into InD or OOD. Approaches typically employ uncertainty-based methods or feature space methods.

Uncertainty-based methods include ensembles [1], energy scores [12, 16, 35], density estimation [6, 7], and entropy [60]. Feature space methods involve latent space distances [33, 55] or gradient-based methods [23, 25, 34, 36, 51]. The dual SISOMe approach of Schmidt et al. [48] combines uncertainty and feature space metrics, making it robust across different settings. Joda uses SISOMe for sample selection and extends it with a task adaptive training algorithm, an OOD filtering step, and a score re-balancing.

Open-Set Active Learning: Open-set AL extends the classic AL scenario by incorporating OOD samples in the unlabeled pool. The methodology primarily relies on methods that treat sample selection and OOD filtering separately, requiring one model for classifying InD samples and an additional model for identifying OOD data [10, 11, 39, 40, 44, 64, 72]. For example, Ning et al. [39] used a Gaussian Mixture Model for the AL sample selection and an auxiliary classification model to detect and filter out OOD samples. Joda completely refrains from additional models or data.

Category Discovery: Category discovery assumes an incomplete knowledge of the existing categories in the dataset [4]. All classes are considered to be within the same domain, but not all classes are known a priori. Within this task, approaches share various techniques with OOD detection, such as contrastive learning [13, 56, 59]. To unveil new categories, latent space clustering approaches like k-means [8, 56] or teacher-student approaches [57] are commonly used. Ma et al. [38] introduced the task of Active Category Discovery (AGD), a combination of category discovery and AL, which exclusively queries novel categories.

Concluding, existing works addressing AL and OOD detection do not cover category discovery. Conversely, Ma et al. [38] addressed category discovery but only for novel classes, not for known or OOD data. The combination of AL, OOD detection, and category discovery remains unexplored and will be addressed in this work.

3. Open-Set Discovery Active Learning

This section introduces the novel Open-Set Discovery Active Learning (OSDAL) scenario, combining AL, OOD data, and category discovery. We illustrate this novel scenario in Fig. 1. We begin with a labeled pool L (1) and an unlabeled pool U (3). In each iteration i of the cyclic AL process, a set \mathcal{A} of query size q is chosen from U and sent to an annotator (4). The annotated set \mathcal{A} is then added with its corresponding labels to L for the subsequent cycle, such that $U^{i+1} = U^i \setminus \mathcal{A}$ and $L^{i+1} = L^i \cup \mathcal{A}$. In each cycle, the model (2) f is (re-)trained such that it minimizes the loss over the labeled data, i.e., $f(\omega) : \min_{\omega} \mathcal{L}(x, y)$, where $(x, y) \in (\mathcal{X}_L, \mathcal{Y}_L)$, and \mathcal{X}_L represents the set of labeled samples while \mathcal{Y}_L represents their corresponding labels. This model enables the query strategy $Q(\mathcal{X}, f)$ to choose

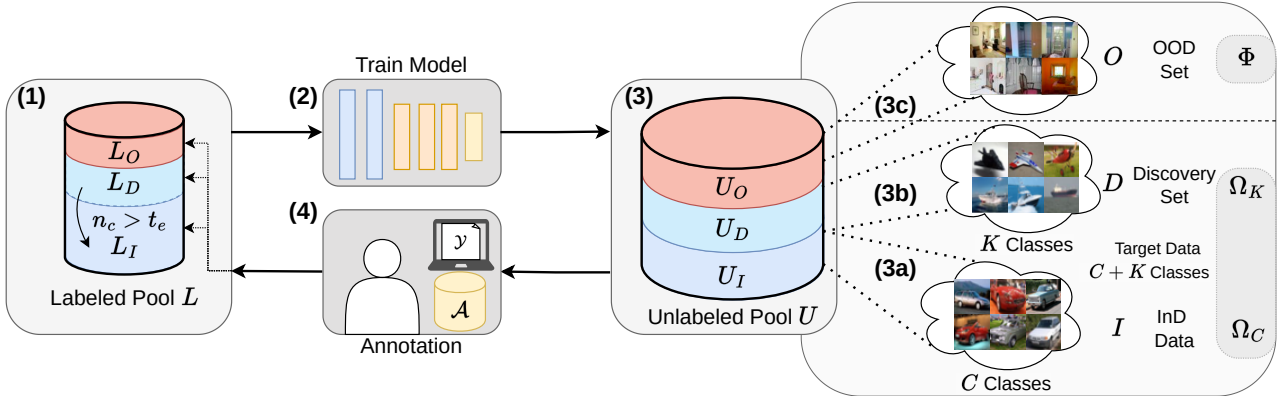


Figure 1. Overview of the Open-Set Discovery Active Learning cycle. Starting with the labeled pool (1) for training a model (2) used to select data from an unlabeled pool (3). Contrasting with previous works, it comprises three subsets: known classes (3a), novel discoverable classes (3b), and unwanted OOD data (3c). After selection, the cycles closed with annotation (4).

data based on the model output or intermediate representation f . We extend the classic AL settings by assuming incomplete relevant class knowledge and OOD data pollution. To do so, we define three sets of data types: the InD data I containing the initial known categories (3a), the discovery set D retaining the novel discoverable categories (3b), and the OOD set O (3c) holding data that belong neither to known nor unknown relevant categories.

To establish the discovery set D and the OOD set O , we orientate on the distinction between near- and far-OOD data commonly employed in OOD benchmarks [63, 70]. Near-OOD data is semantically more similar to InD data, making differentiation more challenging. On the other hand, far-OOD data differs more strongly from InD data, making it easier to distinguish. In the presented scenario, the categories to be discovered are assumed to be related to near-OOD data, while far-OOD data relates to the OOD data. We can consider I and D to be sampled from true category distribution Ω , while only the initial distribution Ω_C containing C categories has been observed given the samples in L . The remaining K categories can be sampled from Ω_K as samples of D and should be discovered throughout the cyclic process, with the number of discoverable classes K remaining unknown. In contrast, we assume far-OOD data to be sampled from a distribution Φ containing irrelevant classes for the application that are neither categorized as any of the $K + C$, which should be filtered out, akin to open-set AL.

As this subset categorization of U is unknown, a query strategy must identify the informative samples in U to unveil the unknown categories and improve the model performance on $C + K$ categories. In each cycle, a set \mathcal{A} of q samples can be selected and sent for annotation (4). Subsequently, these samples are added to the labeled pool L , which is divided into three sub-pools: L_O , containing the selected OOD data identified by the annotator; L_I , comprising samples of already known classes; and L_D , designated

for newly discovered classes where the number of samples n_c is below a threshold t_e . If the sample count of a category reaches the threshold t_e , it will be included in the known classes and transferred to L_I . This threshold simulates a triage process by the annotator to justify the relevance and prevents training instabilities due to a highly unbalanced training set. Alternatively, the threshold can be set to zero, and techniques for strongly unbalanced datasets, such as uniform sampling classes, can be applied. Aligned with the open-set AL scenarios [39], the (accidental) queried OOD data L_O marked by the annotator is available for future use in the next cycle. The extension of the labeled pool L (1) with the queried data \mathcal{A} initiates a new cycle, and the model is retrained.

4. Joint Out-of-Distribution Filtering and Data Discovery Active Learning

Table 1. Overview of existing open-set AL methods, with number of classes K , labeled set L and unlabeled pool U . Additional hyperparameters are separated between metric and models if possible and estimated from the official implementations.

Method	Additional Models	Data Usage	Additional Hyperparameters
LfOSA [39]	1	L	4 + 2
CCAL [11]	2	L & U	2 + 14
MqNet [40]	2 (+1)	L & U	1 + 14
Pal [64]	2	L & U	3 + 9
EOAL [44]	2(+K)	L & U	8
Joda (ours)	0	L	1 + 0

The novel OSDAL scenario requires distinguishing between known I , task-relevant discoverable D samples, and task-irrelevant OOD samples O . As we will show in various experiments, previous works [11, 39, 40, 44] are not fine granular enough for the simultaneous separation of three

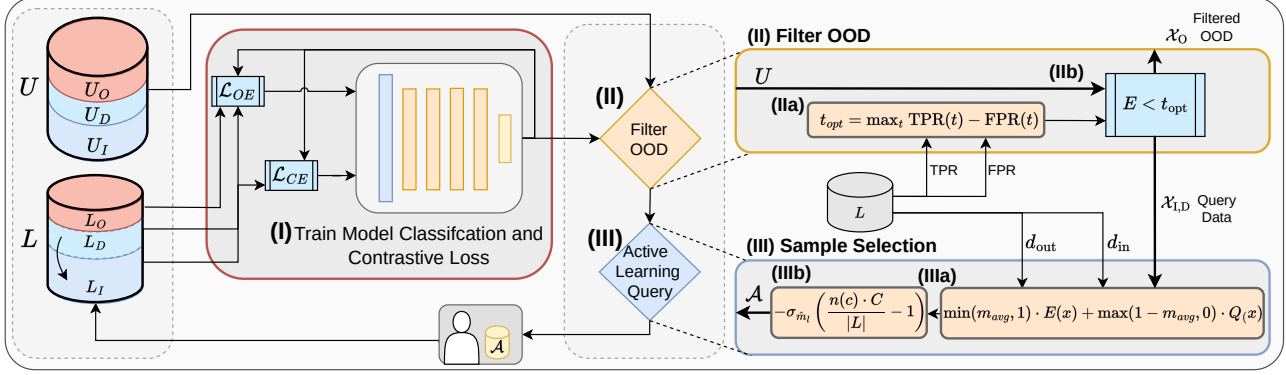


Figure 2. Joint Out-of-Distribution Filtering and Data Discovery Active Learning, comprising of the training phase **(I)** combining classification and outlier exposures loss followed by the filtering **(II)** and selection phase **(III)**. For the filtering, a threshold is estimated on L **(IIa)** to separate OOD samples based on their energy value **(IIb)**. Subsequently, samples are selected based on the SISOME [48] metrics **(IIIa)** combined with a class balancing **(IIIb)**.

sets. In addition, existing methods employ one or more auxiliary models that need to be optimized and mostly require access to the unlabeled pool U . Tab. 1 compares the additional model and data requirements. Optimizing multiple models adds complexity during the training process, especially when U with unknown composition and OOD data is used for training. In addition, it poses a huge limitation in usability for stream-based AL scenarios [46, 53].

We propose Joda to provide a more granular selection strategy for separating I , D , and O simultaneously while eliminating the need for additional models and data. Instead Joda simplifying compared to existing works and addresses the challenges of OSDAL by utilizing a *single model* that is composed of well-coordinated and interdependent components. In Fig. 2, Joda is outlined, comprising of a training **(I)**, filtering **(II)**, and selection **(III)** phase. During the training of the task model **(I)**, Joda utilizes InD and unintentionally selected OOD data to separate both distributions’ feature space representation, improving the subsequent OOD filtering **(II)**. As mentioned before, no auxiliary model is trained during this process. After the model is trained, we conduct an OOD filtering **(II)** leveraging our training scheme and sample selection **(III)** to identify samples for labeling.

Training Phase (I): Prior research in the OOD detection domain only considers the binary separation between InD and OOD. It has not accounted for the threefold separation of InD, near-OOD, and far-OOD data. The challenge in this scenario is to differentiate the unknown sets D and O to avoid mistakenly selecting OOD data or inadvertently dismissing discoverable classes. Since the separation is not infallible, three distinct sets, L_I , L_D , and L_O , may appear in the labeled pool L . Utilizing the existence of O in the labeled pool L , we aim to construct a feature space that groups samples from I and D closer together than samples from O .

To achieve this, we propose a new loss function operation in a polluted labeled pool. We combine an outlier exposure loss [22] \mathcal{L}_{OE} for OOD data L_O within our labeled pool with a Cross-Entropy loss \mathcal{L}_{CE} for the InD part L_I weighted by a hyperparameter λ_{OE} . For each batch, we process the InD part $b_{InD} \subset L_I$ and the OOD part $b_{OOD} \subset L_O$ separately, such that the final loss function can be written as:

$$\begin{aligned} \mathcal{L}(b) &= \mathcal{L}_{CE}(b_{InD}) + \lambda_{OE} \cdot \mathcal{L}_{OE}(b_{OOD}) \\ \mathcal{L}_{OE}(b) &= -\frac{1}{b} \sum_{x \in b} \left(\frac{1}{C} \sum_{i=c}^{C-1} f(x)_i - \log \left(\sum_{i=c}^{C-1} e^{f(x)_i} \right) \right) \end{aligned} \quad (1)$$

With \mathcal{L}_{OE} , we can regularize the model to predict a uniform distribution for OOD instances, which we will exploit in the following phases. Given a pure labeled set L containing only InD data I , the loss collapses to a standard cross-entropy loss.

Separation Phase (II): After completing the training phase, we proceed to the querying phase with the primary objective of filtering out any OOD data before selecting data for labeling. We utilize the energy score, as defined in Eq. (2), as a metric for identifying the OOD samples. This approach leverages from the $\log \sum \exp$ term in Eq. (1).

$$E(x) = -\log \sum_{i=1}^c \exp(f(x)_i) \quad (2)$$

To determine the optimal threshold for identifying OOD data from O , we conduct a Receiver Operating Characteristic (ROC) analysis on the labeled pool L . This analysis helps to calculate the true- and false-positive rates (TPR/FPR) across various thresholds. We then identify the threshold t_{opt} that maximizes Youden’s J statistic [67], which is the difference between TPR and FPR: $t_{opt} = \arg \max \text{TPR}(t) - \text{FPR}(t)$. This optimization identifies the

top-left-most point on the ROC curve, representing the best trade-off between capturing OOD outliers and preserving InD data. Consequently, we classify unlabeled samples x as InD or discoverable if their energy scores are below the threshold $\mathcal{X}_{\text{InD}} = \{x \in U \mid E < t_{\text{opt}}\}$ and as OOD otherwise $\mathcal{X}_{\text{OOD}} = \{x \in U \mid E > t_{\text{opt}}\}$. Given that the initial set L in the first cycle does not contain OOD data, we omit the filtering step and start with the sample selection directly.

Selection Phase (III): After separating the OOD data, we proceed with selecting q samples for labeling. During the selection, it is crucial to balance the exploration of new categories with the selection of valuable samples from known classes. To accomplish this, we employ SISOME [48] as a selection metric, which harnesses the ambiguity of near-OOD and valuable AL samples. It is, therefore, suitable for selecting known and novel categories within the unlabeled pool U . The SISOME score $\hat{m}(x)$ balances the quotient Q of inner and outer class distances d_{in} and d_{out} , and energy score E through a feature space separability value m_{avg} :

$$\begin{aligned} \hat{m}(x) &= \min(m_{\text{avg}}, 1) \cdot E(x) + \max(1 - m_{\text{avg}}, 0) \cdot Q(x) \\ Q(x) &= \frac{d_{\text{in}}(x)}{d_{\text{out}}(x)}; \quad m_{\text{avg}} = \frac{1}{|L|} \sum_x \frac{d_{\text{in}}(x)}{d_{\text{out}}(x)}; \quad x \in \mathcal{X}_{\text{InD}}. \end{aligned} \quad (3)$$

The self-balancing through m_{avg} enables the SISOME score to reflect a diversity, uncertainty trade-off. By evaluating the energy as well as the feature space in \hat{m} , we close the loop to our loss function in Eq. (1). Since D is not included in the objective of Eq. (1), it is not regularized, which promotes the exploration of novel classes. If a class originates from the initial known classes, it accumulates more samples in subsequent cycles compared to a newly revealed class. To address the substantial class imbalance that arises when a new class is introduced, we establish a class-balancing factor $b_f(c)$. By this factor, we aim to weigh the class scores to favor uniform class partitions. We estimate the quotient of the counts per class $n(c)$ by using the currently predicted pseudo-class $\arg \max(f(x))$. We multiply this by the number of classes C and divide it by the size of the labeled pool $|L|$. By subtracting 1, we get a positive score if the number of classes is below their uniform class share $\frac{|L|}{C}$ and a negative if it is above. By scaling with the standard deviation of \hat{m}_l we create the class balance corrected score $\hat{m}_b(x)$:

$$\begin{aligned} \hat{m}_b(x) &= \hat{m}(x) + b_f(\arg \max_c(f(x))) \\ b_f(c) &= -\sigma_{\hat{m}_l} \left(\frac{n(c) \cdot C}{|L|} - 1 \right) \end{aligned} \quad (4)$$

Finally, we select the samples with the highest score $\arg \max_{x \in \mathcal{X}_{\text{InD}}} \hat{m}_b(x)$ according to the query size q . These samples are then sent for annotation which completes the AL cycle.

5. Experiments

Our experiments aim to measure the performance of existing AL approaches and Joda on the proposed OSDAL scenario. To this end, we employ the three standard benchmark sets for open-set AL, namely CIFAR-10, CIFAR-100 [28], and TinyImageNet [9, 31]. In the classic open-set AL setting, the original datasets would be divided into one InD and one OOD dataset. In contrast, for the OSDAL setting, we partition the original dataset into InD I and discovery part D . Moreover, we incorporate an additional dataset to represent the OOD data O . Inspired by [63], we use randomly generated noise samples, MNIST [32], Places365 [71], and ImageNetC-800 [21] with the remaining classes absent in TinyImageNet as OOD data. For Places365, we use the version of OpenOOD [63] which is free of semantic overlaps. Details about the datasets are provided in Appendix A.

Setup: For the experiment settings, we follow the classic AL choices [66] and employ the predominantly used ResNet18 [18] model. To evaluate the InD and discovery performance, we monitor the overall accuracy on target classes, assuming an initial accuracy of 0 for any undiscovered class. This metric effectively gauges the overall performance of the model reflecting class discovery. Furthermore, we calculate the precision score to assess the OOD filtering quality of different algorithms. In the precision calculation, I and D count as positive selection while O counts as negative selection. Finally, we evaluate the number of identified classes during training to measure the discovery capabilities of the methods. Further experiments and additional details regarding experiment setting and hardware, are presented in ?? and Appendix A.

For the comparison, we encompass the following open-set AL baselines: **MQNet** [40], **CCAL** [11], **Pal** [64], and **LfOSA** [39], as well as the classic AL methods, Monte Carlo dropout with entropy (**Ent**) [17], Loss Learning (**LLoss**) [66], **Badge** [2], and **Random**. **EOAL** [44] and **AGD** [38] are not applicable to for OSDAL which we discuss in Appendix A. The open-set AL baselines consider only data from O as OOD in their auxiliary model training to avoid bias against D . To enable a fair comparison, we add OOD samples from O in the initial labeled pool L , which is required by MQNet and CCAL, although Joda and LfOSA can start without them.

CIFAR-100: In Fig. 3, we present our results for CIFAR-100. The columns represent the OOD datasets from left to right: random noise (Random), MNIST, and Places365. The visualizations depict the accuracy, class discovery, and selection precision from top to bottom. The classic AL methods, Ent and LLoss, demonstrate decent performance for random noise as OOD but decrease in performance with the complexity of the OOD data set and get outperformed by others for Places365. Badge, which incorporates diversity, achieves decent overall performance in

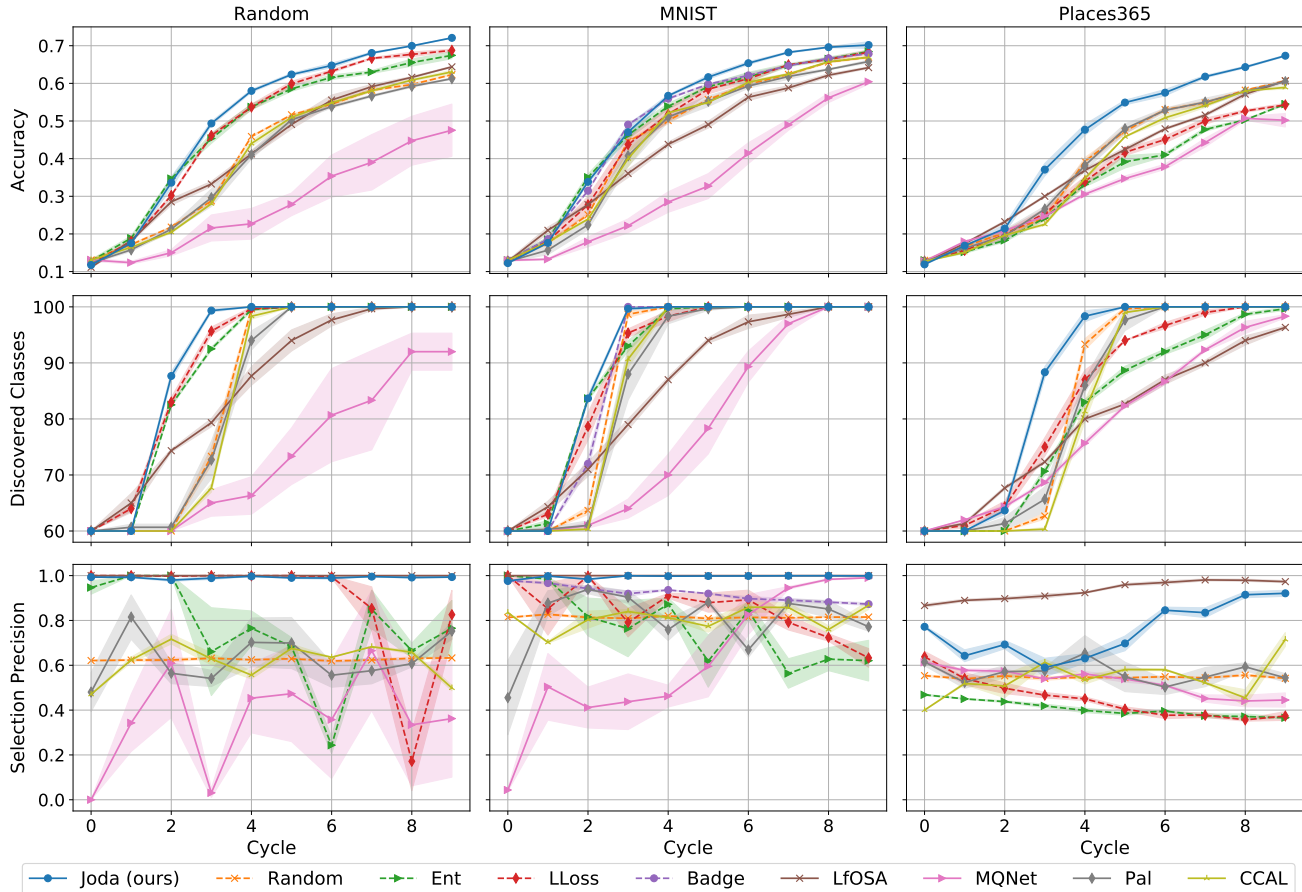


Figure 3. Comparison for CIFAR-100 with ResNet18 and indicated standard errors. From top to bottom: Mean Accuracy, Class Detection, and Selection Precision. OOD datasets from left to right: Random, MNIST, and Places365

OOD datasets. Given that the cubic computing complex depends on the number of classes and samples, Badge is not reported for Places365 and random noise due to memory issues. Additionally, classic AL methods produce inconsistent results for precision selection. However, together with Random selection, they benefit from a small OOD ratio, as in the case of MNIST. Notably, the open-set methods based on contrastive learning CCAL and MQNet achieve inconsistent results. CCAL performs well for MNIST and Places365, while MQNet has difficulties with OOD Random and MNIST. For Places365, MQNet achieves good performance and class separation but suffers in selection precision. LfOSA, utilizing an additional classifier, demonstrates good precision but struggles with class discovery. However, Pal, CCAL, and MQNet improve their selection precision but do not surpass LfOSA or Joda in this aspect.

For all datasets, Joda exhibits a strong performance and consistently outperforms all other methods. In the first one or two cycles, Joda needs a warmup. In all other cycles, Joda shows an early class discovery with stable selection precision. For the easier OOD data, random noise and MNIST, Joda show an almost perfect section precision of

1, while detecting novel categories as fastest method.

TinyImageNet: In Fig. 4, we evaluate our scenario on the more complex TinyImageNet dataset. These experiments present the most difficult setting. The ImageNetC-800 dataset has no semantic overlap and covariate shift to TinyImageNet. The Places365 contains a minor semantic overlap with a different image style as a covariate shift, showcasing the boundaries of the ODSAL scenario. LLoss and Ent perform well for the rather artificial OOD data MNIST. While LLoss can maintain performance for ImageNetC-800 and Places365, Ent falls behind. MQNet manages high precision and selection accuracy for MNIST but drops in more realistic settings. The increased amount of samples and classes leads to issues when computing Badge. LfOSA, Pal, and CCAL achieve high selection precision but struggle with class discovery. Specifically, CCAL has issues with unveiling classes. Remarkably, Joda achieves an almost perfect selection precision of 1.0 in every cycle over all OOD datasets. Accompanied by this Joda shows the fastest class discovery. For the higher resolution ImageNet dataset, Joda gets in a competition for the easily distinguishable dataset MNIST. For the more realis-

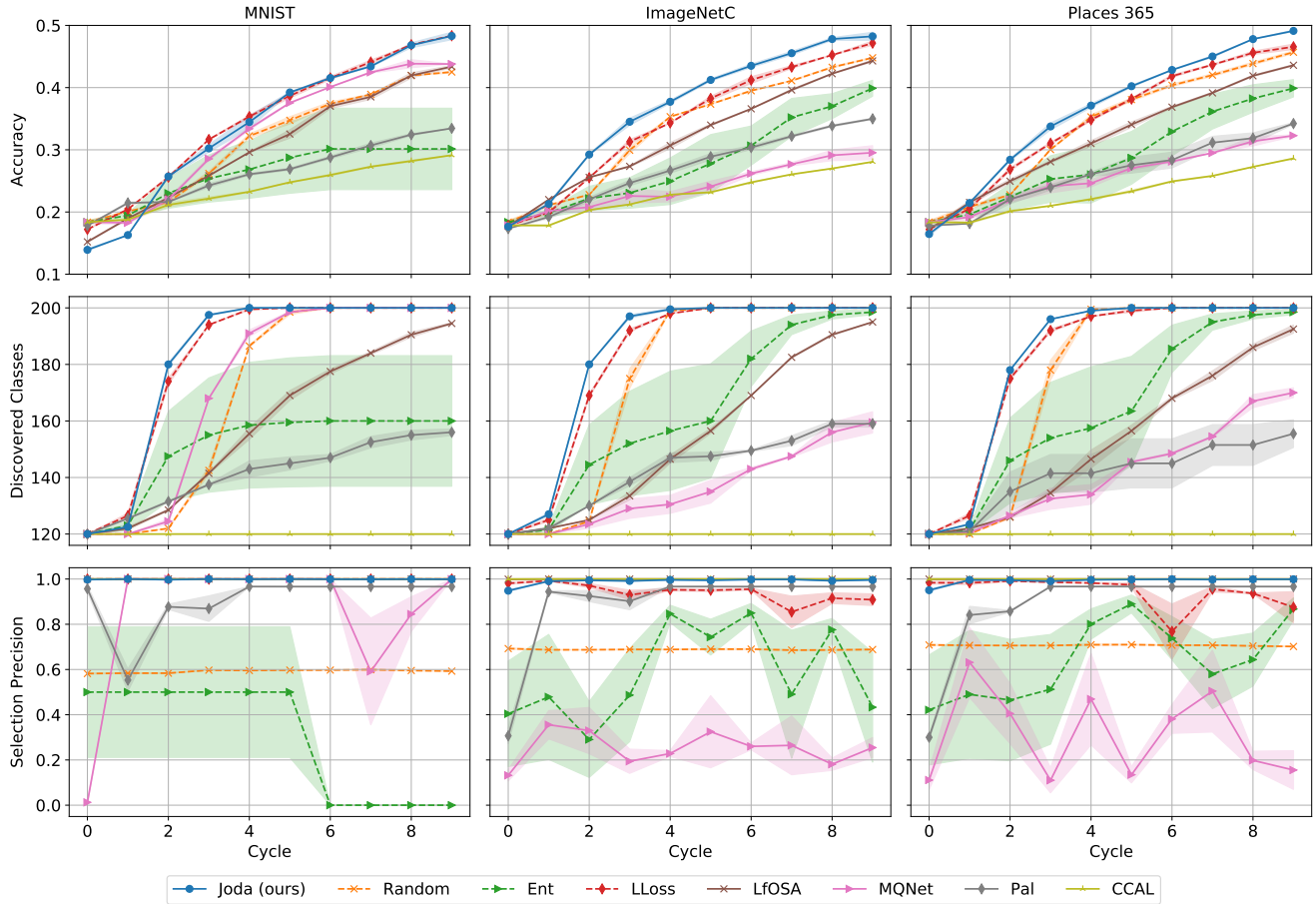


Figure 4. Comparison for TinyImageNet with ResNet18 and indicated standard errors. From top to bottom: Accuracy, Class Detection, and Selection Precision. OOD datasets from left to right: MNIST, ImageNetC-800, and Places365.

tic ImageNetC-800 Joda reaches the highest accuracy. Even for the minor covariate shift of Places365 Joda maintains its strong performance in accuracy, class discovery, and selection precision. In Appendix D we report an additional experiment with random noise as OOD data. Given the higher image resolution, the experiment shows behavior similar to that of MNIST.

CIFAR-10: Lastly, we perform experiments on CIFAR-10, the most commonly used AL benchmark. Compared to CIFAR-100 and TinyImageNet, it has a much lower number of classes. In Fig. 11 in Appendix G, we conduct the same experiment setup as for CIFAR-100. Compared to the CIFAR-100, the margins between the methods decrease, creating competition in the first cycles. Lastly, Joda can achieve the highest accuracy over all OOD data sets. Again, it achieves for random noise and MNIST a selection precision of almost 1 while discovering all classes as first.

Additional Models: In Appendix B, we evaluate the transferability of Joda to a different model. For ResNet50, Joda can obtain a similar performance as delivered in Fig. 3, enabling Joda to achieve the highest performance.

Scenario Variation: Besides the complexity of the dataset, the number and proportion of known and discoverable categories significantly impact method behavior. In Appendix C, we evaluate the different InD to OOD ratios, different InD to novel categories ratios as well as an imbalance in number of samples per class. We analyze varying amounts of initially known categories in Fig. 7, where Joda shows a consistent performance over different rates. In experiments varying the InD to OOD setting in Fig. 8, Joda can continue its high performance, such that Joda shows a robust behavior for different InD, novel categories, and OOD ratios. In the unbalanced setting in Fig. 10, Joda shows is robustness against other methods in this setting and increases the gap to other methods compared to Fig. 3. In addition, in this setting the effect of the balancing factor introduced in Eq. (4) reviles it full advantage and is analyzed.

Different Query Sizes: The effect of different query sizes is analyzed in Appendix E where Joda remains performant over different selection size variations.

Ablation Study: In our ablation study, we investigate the different components of Joda, as well as different hy-

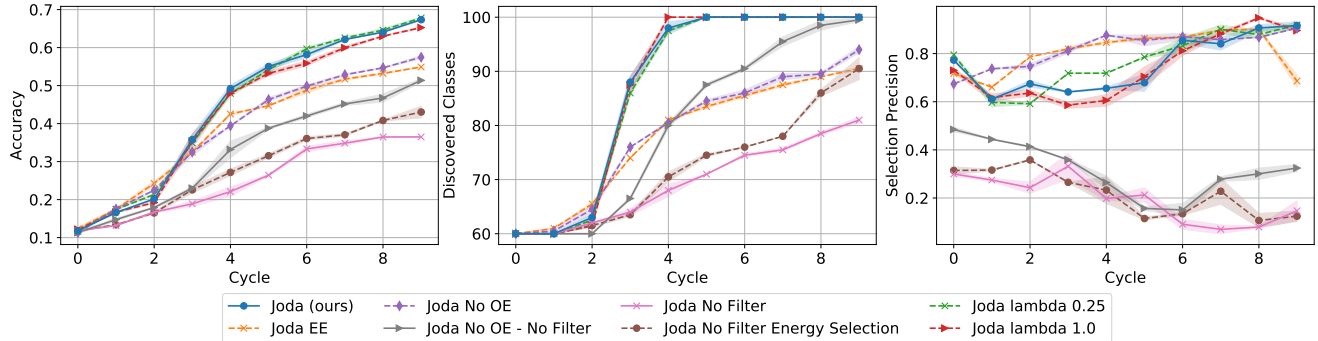


Figure 5. Ablation study on Joda using ResNet18 and CIFAR-100 and Places365 with indicated standard errors.

perparameter settings. In Fig. 5, we omitted the OE component in Eq. (1), replaced it with an Energy Exposure (EE) [35] component, and removed the energy-based filtering step (No OE - No Filter). The OE and the critical components of filtering heavily affect class discovery and selection precision and accuracy. The direct energy regularization by an EE loss component performs worse than the OE. Removing the OOD filtering and replacing the SISOME selection with a pure energy-based selection show significant drops in accuracy, class discovery, and selection precision. This underlines the deep entanglement of all components of Joda leading to a strong performance. In addition, we compare with different values for the hyperparameter λ in Eq. (1) with the value of 0.5 chosen for Joda. It can be seen that Joda shows, in general, a robust behavior against hyperparameter changes, and different variations of λ have only a minor impact on the performance of Joda.

Over all experiments, we observed a suitable performance of uncertainty-based classic AL methods for CIFAR-10 and CIFAR-100, especially LLoss, which reported a strong performance for easy OOD data and also for TinyImageNet. For Ent, we assume that smaller variation for far-OOD data leads to good filtering properties. Driven by the auxiliary open-set classifier, LfOSA consistently achieved high selection precision, which comes at the cost of a reduced class discovery. The open-set methods CCAL and MQNet employ multiple auxiliary models and achieve an inconsistent performance for the different dataset combinations, underlining the sensitivity of contrastively trained auxiliary models. Pal manages to maintain a good trade-off between exploration and selection precision. CCAL, MQNet, and Pal struggle to distinguish OOD data from InD data if it comes from a different dataset source. In 8 out of 10 combinations, Joda achieves a selection precision of almost 1.0 while providing the fastest class discovery in all settings. In the 2 remaining settings, the only method showing a higher selection precision cannot unveil all unknown classes. Additionally, for 14 combinations, Joda achieves the highest accuracy and only ranks second for TinyImageNet with Random noise at a perfor-

mance similar to the best competitor. It should be noted that especially for the most complex and realistic OOD datasets, Places365 and ImageNetC-800, Joda consistently reports the best accuracy over all three InD datasets. In variation scenarios, examining different InD to OOD and InD to novel class ratios, Joda shows a consistent performance regardless of the ratio. The consistent performance of Joda, when different hyperparameters are applied, makes it easily transferable to more scenarios.

Limitations: The generality of our novel problem framework, OSDAL, allows for a vast range of benchmarking opportunities. While we believe that we present the most relevant evaluation, we acknowledge that future research may expand upon our work through additional datasets and OOD scenarios.

6. Conclusion

To address AL in real-world applications like autonomous driving or environmental perception, where prior knowledge of the unlabeled data is absent, we propose *Open-Set Discovery Active Learning* (OSDAL). OSDAL combines AL with the open-world challenges of OOD detection and category discovery, providing an extension of open-set AL. We overcome these challenges by presenting **Joint Out-of-distribution filtering and data Discovery Active Learning** (Joda). Joda is the first AL approach with a selection capable of simultaneously filtering OOD and class discovery. Additionally, Joda eliminates the need for additional models required by existing open-set AL approaches. Furthermore, Joda only uses data from the labeled pool for training. These properties make Joda lightweight and easy to apply. In an extensive evaluation comprising 15 scenarios 3 metrics and 8 competitors over a wide range of datasets, Joda consistently achieved the highest scores.

In future work, we aim to explore further settings and extend OSDAL and Joda to more complex tasks with complex novel class behavior like semantic segmentation or object detection.

References

- [1] Devansh Arpit, Huan Wang, Yingbo Zhou, and Caiming Xiong. Ensemble of averages: Improving model selection and boosting performance in domain generalization. In *Proceedings of the International Conference on Neural Information Processing Systems (NeurIPS)*, 2022. 2
- [2] Jordan T Ash, Chicheng Zhang, Akshay Krishnamurthy, John Langford, and Alekh Agarwal. Deep batch active learning by diverse, uncertain gradient lower bounds. In *Proceedings of the International Conference on Learning Representations (ICLR)*, 2020. 2, 5, 1, 4
- [3] William H Beluch, Tim Genewein, Andreas Nürnberger, and Jan M Köhler. The power of ensembles for active learning in image classification. In *Proceedings of the IEEE/CVF Conference on Computer Vision and Pattern Recognition (CVPR)*, 2018. 2
- [4] Kaidi Cao, Maria Brbić, and Jure Leskovec. Open-world semi-supervised learning. In *Proceedings of the International Conference on Learning Representations (ICLR)*, 2022. 2
- [5] Razvan Caramalau, Binod Bhattarai, and Tae-Kyun Kim. Sequential graph convolutional network for active learning. In *Proceedings of the IEEE/CVF Conference on Computer Vision and Pattern Recognition (CVPR)*, 2021. 2, 1
- [6] Bertrand Charpentier, Daniel Zügner, and Stephan Günnemann. Posterior network: Uncertainty estimation without ood samples via density-based pseudo-counts. In *Proceedings of the International Conference on Neural Information Processing Systems (NeurIPS)*, 2020. 2
- [7] Bertrand Charpentier, Oliver Borchert, Daniel Zügner, Simon Geisler, and Stephan Günnemann. Natural posterior network: Deep bayesian uncertainty for exponential family distributions. In *International Conference on Machine Learning (ICML)*, 2022. 2
- [8] Florent Chieroni, Jose DolzÉTS Dolz, DolzÉTS Montreal Montreal, Canada Ziko Imtiaz Masud, Ismail Ben AyedÉTS Ayed, and AyedÉTS Montreal Montreal. Parametric information maximization for generalized category discovery. In *Proceedings of the IEEE/CVF International Conference on Computer Vision (ICCV)*, 2023. 2
- [9] Jia Deng, Wei Dong, Richard Socher, Li-Jia Li, Kai Li, and Li Fei-Fei. Imagenet: A large-scale hierarchical image database. In *Proceedings of the IEEE/CVF Conference on Computer Vision and Pattern Recognition (CVPR)*, 2009. 5
- [10] Pan Du, Suyun Zhao, Hui Chen, Shuwen Chai, Hong Chen, and Cuiping Li. Contrastive coding for active learning under class distribution mismatch. In *Proceedings of the IEEE/CVF International Conference on Computer Vision (ICCV)*, 2021. 2, 1, 5
- [11] Pan Du, Hui Chen, Suyun Zhao, Shuwen Chai, Hong Chen, and Cuiping Li. Contrastive active learning under class distribution mismatch. *IEEE Transactions on Pattern Analysis and Machine Intelligence*, 45:4260–4273, 2023. 1, 2, 3, 5
- [12] Sven Elfle, Bertrand Charpentier, Daniel Zügner, and Stephan Günnemann. On out-of-distribution detection with energy-based models. *arXiv*, 2107.08785, 2021. 2
- [13] Yixin Fei, Zhongkai Zhao, Siwei Yang, and Bingchen Zhao. Xcon: Learning with experts for fine-grained category discovery. In *Proceedings of the British Machine Vision Conference (BMVC)*, 2022. 2
- [14] Di Feng, Xiao Wei, Lars Rosenbaum, Atsuto Maki, and Klaus Dietmayer. Deep active learning for efficient training of a lidar 3d object detector. In *Proceedings of the IEEE Intelligent Vehicles Symposium (IV)*, 2019. 2
- [15] Dominik Fuchsgruber, Tom Wollschläger, Bertrand Charpentier, Antonio Oroz, and Stephan Günnemann. Uncertainty for active learning on graphs. *Arxiv*, 2405.01462, 2024. 2
- [16] Dominik Fuchsgruber, Tom Wollschläger, and Stephan Günnemann. Energy-based epistemic uncertainty for graph neural networks. *Arxiv*, 2406.04043, 2024. 2
- [17] Yarin Gal and Zoubin Ghahramani. Dropout as a bayesian approximation: Representing model uncertainty in deep learning. In *Proceedings of the International Conference on Machine Learning (ICML)*, 2016. 2, 5, 4
- [18] Kaiming He, Xiangyu Zhang, Shaoqing Ren, and Jian Sun. Deep residual learning for image recognition. In *Proceedings of the IEEE/CVF Conference on Computer Vision and Pattern Recognition (CVPR)*, 2016. 5, 1
- [19] Aral Hekimoglu, Michael Schmidt, Alvaro Marcos-Ramiro, and Gerhard Rigoll. Efficient active learning strategies for monocular 3d object detection. In *Proceedings of the IEEE Intelligent Vehicles Symposium (IV)*, 2022. 2
- [20] Aral Hekimoglu, Michael Schmidt, and Alvaro Marcos-Ramiro. Monocular 3d object detection with lidar guided semi supervised active learning. In *Proceedings of the IEEE/CVF Winter Conference on Applications of Computer Vision (WACV)*, 2024. 2
- [21] Dan Hendrycks and Thomas Dietterich. Benchmarking neural network robustness to common corruptions and perturbations. In *ICLR*, 2019. 5, 1
- [22] Dan Hendrycks and Kevin Gimpel. A baseline for detecting misclassified and out-of-distribution examples in neural networks. In *Proceedings of the International Conference on Learning Representations (ICLR)*, 2016. 4
- [23] Yen-Chang Hsu, Yilin Shen, Hongxia Jin, and Zsolt Kira. Generalized odin: Detecting out-of-distribution image without learning from out-of-distribution data. In *Proceedings of the IEEE/CVF Conference on Computer Vision and Pattern Recognition (CVPR)*, 2020. 2
- [24] Po Yu Huang, Wan Ting Hsu, Chun Yueh Chiu, Ting Fan Wu, and Min Sun. Efficient uncertainty estimation for semantic segmentation in videos. In *Proceedings of the European Conference on Computer Vision (ECCV)*, 2018. 2
- [25] Rui Huang, Andrew Geng, and Yixuan Li. On the importance of gradients for detecting distributional shifts in the wild. In *Proceedings of the International Conference on Neural Information Processing Systems (NeurIPS)*, 2021. 2
- [26] Kwanyoung Kim, Dongwon Park, Kwang In Kim, and Se Young Chun. Task-aware variational adversarial active learning. In *Proceedings of the IEEE/CVF Conference on Computer Vision and Pattern Recognition (CVPR)*, 2021. 2, 1
- [27] Andreas Kirsch, Joost Van Amersfoort, and Yarin Gal. Batchbald: Efficient and diverse batch acquisition for deep

- bayesian active learning. In *Proceedings of the International Conference on Neural Information Processing Systems (NeurIPS)*, 2019. 2
- [28] Alex Krizhevsky, Vinod Nair, and Geoffrey Hinton. Learning multiple layers of features from tiny images. Technical report, Canadian Institute for Advanced Research, 2009. 5, 1
- [29] kuangliu. pytorch-cifar, 2021. 1
- [30] Balaji Lakshminarayanan, Alexander Pritzel, and Charles Blundell. Simple and scalable predictive uncertainty estimation using deep ensembles. In *Proceedings of the International Conference on Neural Information Processing Systems (NeurIPS)*, 2017. 2
- [31] Ya Le and Xuan Yang. Tiny imagenet visual recognition challenge. Technical Report 7, Stanford Computer Vision Lab, 2015. 5, 1
- [32] Yann LeCun, Léon Bottou, Yoshua Bengio, and Patrick Haffner. Gradient-based learning applied to document recognition. In *Proceedings of the IEEE*, 1998. 5
- [33] Kimin Lee, Kibok Lee, Honglak Lee, and Jinwoo Shin. A simple unified framework for detecting out-of-distribution samples and adversarial attacks. In *Proceedings of the International Conference on Neural Information Processing Systems (NeurIPS)*, 2018. 2
- [34] Shiyu Liang, Yixuan Li, and R Srikant. Enhancing the reliability of out-of-distribution image detection in neural networks. In *Proceedings of the International Conference on Learning Representations (ICLR)*, 2018. 2
- [35] Weitang Liu, Xiaoyun Wang, John D. Owens, and Yixuan Li. Energy-based out-of-distribution detection. In *Proceedings of the International Conference on Neural Information Processing Systems (NeurIPS)*, 2020. 2, 8
- [36] Yibing Liu, Chris Xing Tian, Haoliang Li, Lei Ma, and Shiqi Wang. Neuron activation coverage: Rethinking out-of-distribution detection and generalization. In *Proceedings of the International Conference on Learning Representations (ICLR)*, 2024. 2
- [37] Yadan Luo, Zhuoxiao Chen, Zijian Wang, Xin Yu, Zi Huang, and Mahsa Baktashmotlagh. Exploring active 3d object detection from a generalization perspective. In *Proceedings of the International Conference on Learning Representations (ICLR)*, 2023. 2
- [38] Shijie Ma, Fei Zhu, Zhun Zhong, Xu-Yao Zhang, and Cheng-Lin Liu. Active generalized category discovery. *Arxiv*, 2403.04272, 2024. 2, 5, 1
- [39] Kun-Peng Ning, Xun Zhao, Yu Li, and Sheng-Jun Huang. Active learning for open-set annotation. In *CVPR*, 2022. 1, 2, 3, 5
- [40] Dongmin Park, Yooju Shin, Jihwan Bang, Youngjun Lee, Hwanjun Song, and Jae-Gil Lee. Meta-query-net: Resolving purity-informativeness dilemma in open-set active learning. In *Neurips*, 2022. 1, 2, 3, 5
- [41] Younghyun Park, Wonjeong Choi, Soyeong Kim, Dong-Jun Han, and Jaekyun Moon. Active learning for object detection with evidential deep learning and hierarchical uncertainty aggregation. In *Proceedings of the International Conference on Learning Representations (ICLR)*, 2023. 2
- [42] Adam Paszke, Sam Gross, Francisco Massa, Adam Lerer, James Bradbury, Gregory Chanan, Trevor Killeen, Zeming Lin, Natalia Gimelshein, Luca Antiga, Alban Desmaison, Andreas Kopf, Edward Yang, Zachary DeVito, Martin Raison, Alykhan Tejani, Sasank Chilamkurthy, Benoit Steiner, Lu Fang, Junjie Bai, and Soumith Chintala. Pytorch: An imperative style, high-performance deep learning library. In *Proceedings of the International Conference on Neural Information Processing Systems (NeurIPS)*, pages 8024–8035. 2019. 1
- [43] Fengchao Peng, Chao Wang, Jianzhuang Liu, Zhen Yang Noah, and Ark Lab. Active learning for lane detection: A knowledge distillation approach. In *Proceedings of the IEEE/CVF International Conference on Computer Vision (ICCV)*, 2021. 2
- [44] Bardia Safaei, Vibashan VS, Celso M. de Melo, and Vishal M. Patel. Entropic open-set active learning. In *AAAI*, 2024. 1, 2, 3, 5
- [45] Mohammadreza Salehi, Hossein Mirzaei, Dan Hendrycks, Yixuan Li, Mohammad Hossein Rohban, and Mohammad Sabokrou. A unified survey on anomaly, novelty, open-set, and out-of-distribution detection: Solutions and future challenges. *Transaction on Machine Learning (TMLR)*, 2022. 2
- [46] Sebastian Schmidt and Stephan Günnemann. Stream-based active learning by exploiting temporal properties in perception with temporal predicted loss. In *Proceedings of the British Machine Vision Conference (BMVC)*, 2023. 2, 4
- [47] Sebastian Schmidt, Qing Rao, Julian Tatsch, and Alois Knoll. Advanced active learning strategies for object detection. In *Proceedings of the IEEE Intelligent Vehicles Symposium (IV)*, 2020. 2
- [48] Sebastian Schmidt, Leonard Schenk, Leonard Schwinn, and Stephan Günnemann. A unified approach towards active learning and out-of-distribution detection. *arXiv*, 2405.11337, 2024. 2, 4, 5, 1
- [49] Sebastian Schmidt, Lukas Stappen, Leo Schwinn, and Stephan Günnemann. Generalized synchronized active learning for multi-agent-based data selection on mobile robotic systems. *IEEE Robotics and Automation Letters*, 9 (10):8659–8666, 2024. 2
- [50] Sebastian Schmidt, Ludwig Stumpp, Diego Valverde, and Stephan Günnemann. Deep sensor fusion with constraint safety bounds for high precision localization. In *2024 IEEE/RSJ International Conference on Intelligent Robots and Systems (IROS)*, pages 12256–12262. IEEE, 2024. 1
- [51] Leo Schwinn, An Nguyen, René Raab, Leon Bungert, Daniel Tenbrinck, Dario Zanca, Martin Burger, and Bjoern Eskofier. Identifying untrustworthy predictions in neural networks by geometric gradient analysis. In *Conference on Uncertainty in Artificial Intelligence (UAI)*, 2021. 2
- [52] Ozan Sener and Silvio Savarese. Active learning for convolutional neural networks: A core-set approach. In *Proceedings of the International Conference on Learning Representations (ICLR)*, 2018. 2
- [53] Burr Settles. Active learning literature survey. Technical report, University of Wisconsin–Madison, 2010. 1, 2, 4
- [54] Samarth Sinha, Sayna Ebrahimi, and Trevor Darrell. Variational adversarial active learning. In *Proceedings of the*

- IEEE/CVF International Conference on Computer Vision (ICCV)*, 2019. 2
- [55] Yiyu Sun, Yifei Ming, Xiaojin Zhu, and Yixuan Li. Out-of-distribution detection with deep nearest neighbors. In *Proceedings of the International Conference on Machine Learning (ICML)*, 2022. 2
- [56] Sagar Vaze, Kai Han, Andrea Vedaldi, and Andrew Zisserman. Generalized category discovery. In *Proceedings of the IEEE/CVF Conference on Computer Vision and Pattern Recognition (CVPR)*, 2023. 1, 2
- [57] Sagar Vaze, Andrea Vedaldi, and Andrew Zisserman. No representation rules them all in category discovery. In *Proceedings of the International Conference on Neural Information Processing Systems (NeurIPS)*, 2023. 2
- [58] weiaicunzai. pytorch-cifar100, 2022. 1
- [59] Xin Wen, Bingchen Zhao, and Xiaojuan Qi. Parametric classification for generalized category discovery: A baseline study classification objectives. In *Proceedings of the IEEE/CVF International Conference on Computer Vision (ICCV)*, 2023. 2
- [60] C. Zach X. Liu, Y. Lochman. Gen: Pushing the limits of softmax-based out-of-distribution detection. In *Proceedings of the IEEE/CVF Conference on Computer Vision and Pattern Recognition (CVPR)*, 2023. 2
- [61] Chenhongyi Yang, Lichao Huang, and Elliot J. Crowley. Plug and play active learning for object detection. *arXiv*, 2211.11612, 2022. 2
- [62] Jingkan Yang, Kaiyang Zhou, Yixuan Li, and Ziwei Liu. Generalized out-of-distribution detection: A survey. *arXiv*, 2110.11334, 2021. 2
- [63] Jingkan Yang, Pengyun Wang, Dejian Zou, Zitang Zhou, Kunyuan Ding, WenXuan Peng, Haoqi Wang, Guangyao Chen, Bo Li, Yiyu Sun, Xuefeng Du, Kaiyang Zhou, Wayne Zhang, Dan Hendrycks, Yixuan Li, and Ziwei Liu. Openood: Benchmarking generalized out-of-distribution detection. In *Proceedings of the International Conference on Neural Information Processing Systems (NeurIPS) Datasets and Benchmarks Track*, 2022. 3, 5, 1
- [64] Yang Yang, Yuxuan Zhang, Xin Song, and Yi Xu. Not all out-of-distribution data are harmful to open-set active learning. In *Proceedings of the International Conference on Neural Information Processing Systems (NeurIPS)*, 2023. 1, 2, 3, 5
- [65] Ofer Yehuda, Avihu Dekel, Guy Hacohen, and Daphna Weinshall. Active learning through a covering lens. In *Proceedings of the International Conference on Neural Information Processing Systems (NeurIPS)*, 2022. 2
- [66] Donggeun Yoo and In So Kweon. Learning loss for active learning. In *Proceedings of the IEEE/CVF Conference on Computer Vision and Pattern Recognition (CVPR)*, 2019. 2, 5, 1, 4
- [67] W. J. Youden. Index for rating diagnostic tests. *Cancer*, 3(1):32–35, 1950. 4
- [68] Xueying Zhan, Qingzhong Wang, Kuan hao Huang, Haoyi Xiong, Dejing Dou, and Antoni B. Chan. A comparative survey of deep active learning. *Arxiv*, 2203.13450, 2022. 2
- [69] Beichen Zhang, Liang Li, Shijie Yang, Shuhui Wang, Zheng-Jun Zha, and Qingming Huang. State-relabeling adversarial active learning. In *Proceedings of the IEEE/CVF Conference on Computer Vision and Pattern Recognition (CVPR)*, 2020. 2
- [70] Jingyang Zhang, Jingkan Yang, Pengyun Wang, Haoqi Wang, Yueqian Lin, Haoran Zhang, Yiyu Sun, Xuefeng Du, Kaiyang Zhou, Wayne Zhang, Yixuan Li, Ziwei Liu, Yiran Chen, and Hai Li. Openood v1.5: Enhanced benchmark for out-of-distribution detection. In *Proceedings of the International Conference on Neural Information Processing Systems (NeurIPS) Workshop on Distribution Shifts: New Frontiers with Foundation Models*, 2023. 3
- [71] Bolei Zhou, Agata Lapedriza, Aditya Khosla, Aude Oliva, and Antonio Torralba. Places: A 10 million image database for scene recognition. *IEEE Transactions on Pattern Analysis and Machine Intelligence*, 2017. 5
- [72] Chen-Chen Zong, Ye-Wen Wang, Kun-Peng Ning, Hai-Bo Ye, and Sheng-Jun Huang. Bidirectional uncertainty-based active learning for open-set annotation. In *ECCV*, 2024. 2

Joint Out-of-Distribution Filtering and Data Discovery Active Learning

Supplementary Material

A. Experimental Details

In this section, we provide an overview of the parameters and implementation details for the methods and experiments conducted. For the full scenario experiments involving Figs. 3, 4 and 11, we initially designated 60% of the dataset classes as InD data, while the remaining classes were considered discoverable. The threshold t_e for adding a novel class from the discovery set D to the InD data I is derived from a uniformly distribution query size. For CIFAR-10 [28], it is set to 100, while for CIFAR-100 [28] and TinyImageNet [31], it is set to 50 and 25, which is slightly higher than the uniformly distributed query size. The classes are enumerated consecutively to the percentage. The same procedure is utilized for respective percentages in Fig. 7. All experiments were conducted with three different seeds. Only the scenario studies and the TinyImageNet experiments were conducted using two seeds. Across all datasets, we employed random horizontal flipping and random cropping with a padding size of 4, following common practices in [5, 26, 66]. Following these works, the initial labeled pool sizes for CIFAR-10 and CIFAR-100 were set to 1000 and 2000, respectively, before filtering out the discoverable classes. For TinyImageNet [31], the size is established at 40 samples per class according to [39]. The query sizes were set to 1000 for CIFAR-10 and 2500 for CIFAR-100 and TinyImageNet. In the case of CIFAR-10 and CIFAR-100, we utilized the same augmentations and initial pool size as Yoo and Kweon [66], specifically employing horizontal flipping and random cropping with a padding of 4. Similar augmentations were applied for TinyImageNet, as they only marginally differed from those examined by Le and Yang [31]. We employed a ResNet18 [18] as the task model, along with the parameters and model modifications advised for the benchmark datasets [29, 58]. These modifications have also been utilized in previous AL works [5, 26, 66]. TinyImageNet, a subset of ImageNet with an image size of (64, 64) and only 200 classes compared to the original 1000 classes, was subject to the same optimizer and scheduler settings as those chosen for CIFAR-10. We trained the task model from scratch for 200 epochs in each cycle and proceeded with the model, achieving the best performance on the validation dataset for evaluation and sample selection.

The method implementations are based on the official repositories of the respective models: LfOSA [39], CCAL [10], Pal [64], and MQNet [40]. We made modifications to the dataloader and dataset definition for the contrastive training in Pal, CCAL, and MQNet, considering only far-

OOD data as OOD data for the method while ignoring discoverable classes. We tried to adhere to the parameters suggested by the authors as much as possible. However, we decided to reduce the number of epochs for CCAL and MQNet to 100 due to the increased dataset size, resulting in increased iterations per epoch. For Badge [2], we also followed the official implementation. Regarding SISOME [48] applied for the selection in Joda, we used the suggested parameters for the sigmoids of 100, 1000, 0.001, and 0.001 and maintained these settings for all experiments. Additionally, we set $\lambda_{OE} = 0.5$ for all experiments.

The methods EOAL [44] and AGD [38] cannot be applied to the OSDAL scenario. EOAL required one additional model per class, which is hard to transfer to unknown classes. AGD focuses on selecting only novel classes and does not select already known classes, which is hard to adapt to select known and novel classes. A naive adaption did not show meaningful results.

Regarding the OOD dataset, we utilized the "randn" function from PyTorch [42] to generate random noise data. The amount of noise OOD data O is chosen to be equal to the amount of InD data I . Additionally, we provided three different sizes of MNIST as OOD dataset: the validation set comprising 10000 images, the complete training set comprising 60000 images, and lastly, we have augmented the training set by rotating the first 40000 images of MNIST, resulting in a dataset of 100000 images. These MNIST datasets stem the OOD data for Fig. 8. Further, the MNIST validation data used for Figs. 3 and 11 as suggested by [63]. For the much larger TinyImageNet dataset in Fig. 4 the MNIST training set was used. For CIFAR-10 and CIFAR-100 in Figs. 3 and 11, the MNIST validation set was utilized as OOD data. For ImageNetC-800 [21], we used the 800 ImageNetC [21] classes, which are not present in TinyImageNet with the motion blur 2 perturbation. All experiments have been conducted on Nvidia V100 GPU with 32 GB RAM and 8 CPU Cores.

B. Additional Model Evaluation

To validate the usability of Joda for different kinds of models, we conducted additional experiments with a ResNet50 for CIFAR-100 with Places365. We present the results in Fig. 6. For the larger model, all methods show a related performance compared to the ResNet18 model in Fig. 3. However, CCAL and LfOSA show less overlap in accuracy. Joda remains in the first place for accuracy and class discovery.

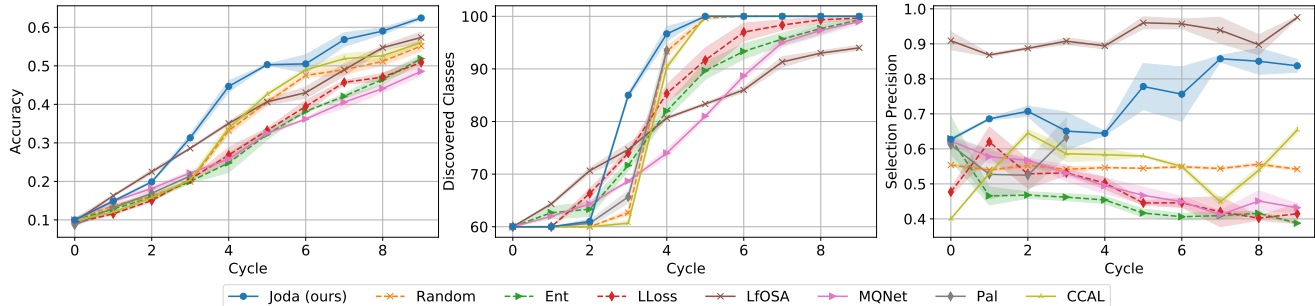


Figure 6. Experiments on ResNet50 and indicated standard errors on CIFAR-100 with Places365.

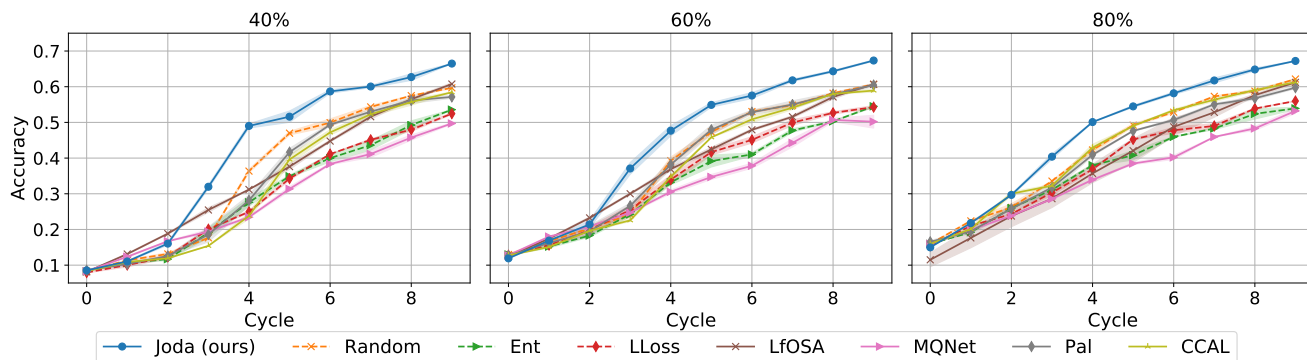


Figure 7. Different InD to discovery set splits with ResNet18 and indicated standard errors on CIFAR-100 with Places365 - InD percentage left to right: 40%, 60% and 80%.

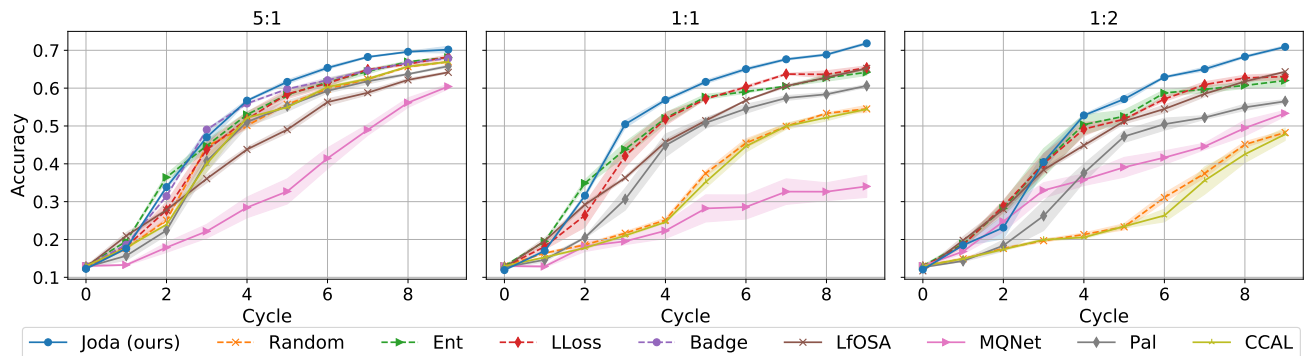


Figure 8. Different InD and OOD ratios with ResNet18 and indicated standard errors on CIFAR-100 with MNIST - InD to OOD ratio left to right: 5:1, 1:1, 1:2.

C. Scenario Variation

To evaluate the effect of different data split ratios, we conduct experiments on the InD to discovery ratios, as well as InD to OOD ratios.

C.1. Varying Discoverable Set Size

Firstly, we analyze varying amounts of initially known categories in Fig. 7. While for 40%, the open-set AL methods maintain a gap to the classic AL methods, the gap decreases

when more data is added. Especially, LfOSA reports a drop for 80% InD classes. Joda maintains the highest performance overall amounts.

C.2. Varying OOD Set Size

Subsequently, we are examining the impact of various OOD dataset sizes. Our experiments with different OOD datasets indicated an influence of the OOD dataset size on the results, particularly for the random selection profits from

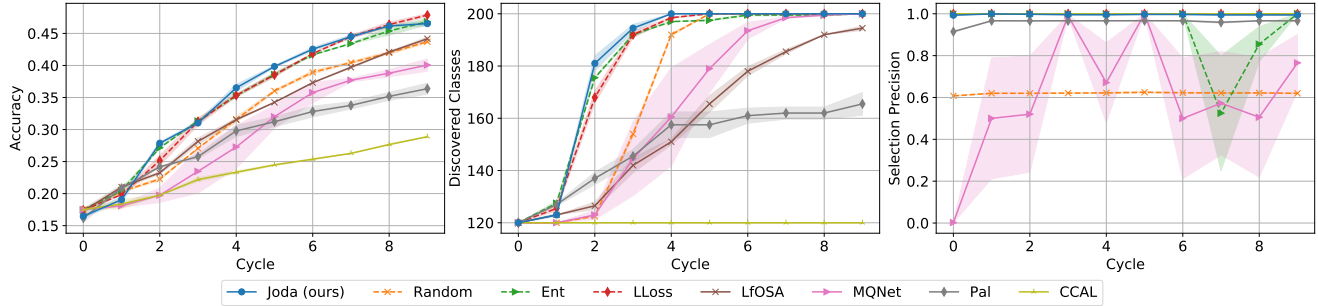


Figure 9. Experiments on ResNet18 and indicated standard errors on TinyImageNet with Random Noise.

low OOD amounts for selection precision. In Fig. 8, we compare different OOD to InD ratios. As expected, the classic AL approach suffers performance drops with rising OOD amounts, while the open-set AL methods, in particular LfOSA, maintain their performance. Joda achieve the highest accuracy over all ratios and extends the margin for increased OOD data. The result underlines the robust behavior of Joda for various dataset splits.

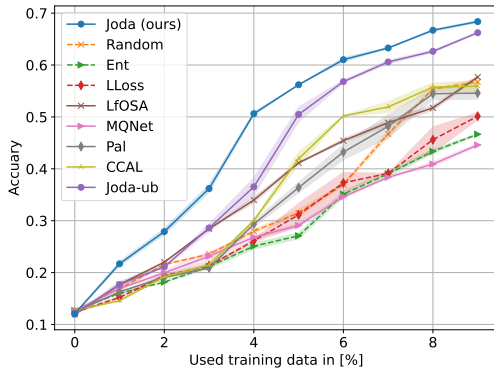


Figure 10. Comparison of an U_I to U_D ratio of 2:1 for CIFAR-100 and Places365 with indicated standard errors using ResNet18.

C.3. Unbalanced Class Samples

In the most experimental setting, the number of samples of already known and discoverable classes are roughly equal. However, in some scenarios, the number of samples of discoverable classes might be lower as they have not been revealed yet. In Fig. 10, we compare the different methods a setting where the discoverable classes are less frequent. It can be seen that Joda shows a strong resistance to the unbalanced classes and increases the gap to the setting of Places365 shown in Fig. 3. In addition, to our Joda we show, the effect of our novel introduced balancing in Eq. (4). Joda-ub presents the unbalanced version, without this factor. While Joda-ub manages to outperforms other AL methods, there remains still a gap to Joda.

D. Further TinyImageNet Experiments

In addition to the experiments conducted in Sec. 5, where we evaluate TinyImageNet with MNIST, ImageNetC-800, and Places365, we examine the behavior for random noise. In Fig. 9, we present these results with accuracy, class discovery, and selection precision. Compared to CIFAR-10 and CIFAR-100 presented in Fig. 11 and Fig. 3, AL approaches and Joda perform much better in terms of accuracy as well as selection precision. Given the larger and more realistic samples, random noise behaves much more abnormal, which can be easier detected by metrics instead of learned latent spaces. In this experiments Joda achieved a the highest class discovery with a perfect selection precision of 1. In cycles 2-8 Joda reports the highest accuracy and is only slightly eclipsed in the last cycle and in the starting cycles where the data is not explored yet. In general, Joda achieves top performance for all three metrics in almost all measurement points.

E. Effect of Selection Size

An essential aspect of AL is the number of selected samples per cycle. The commonly used setting selects 2500 samples for CIFAR-100 as highlighted in Appendix A. While most work in open-set AL do not investigate, this influence of varying selection sizes we investigate the effects of a lower and higher selection size in Fig. 13. In can be seen, that Joda shows in general a high performance over all selection sizes and maintains the difference to other methods. Based on the entanglement of training and filtering, higher selection ratios lead a faster increase of selection precision.

F. Ablation Study on Selection Method

While Joda entangles the training, filtering and selection in an enhanced manner to avoid additional data access and axillary model or ensemble requirement, its structure remains flexible. Based by this design Joda remains open to methods improvements. In Fig. 12, we replace the selection of Joda by and MC Dropout Entropy selection. While it can be

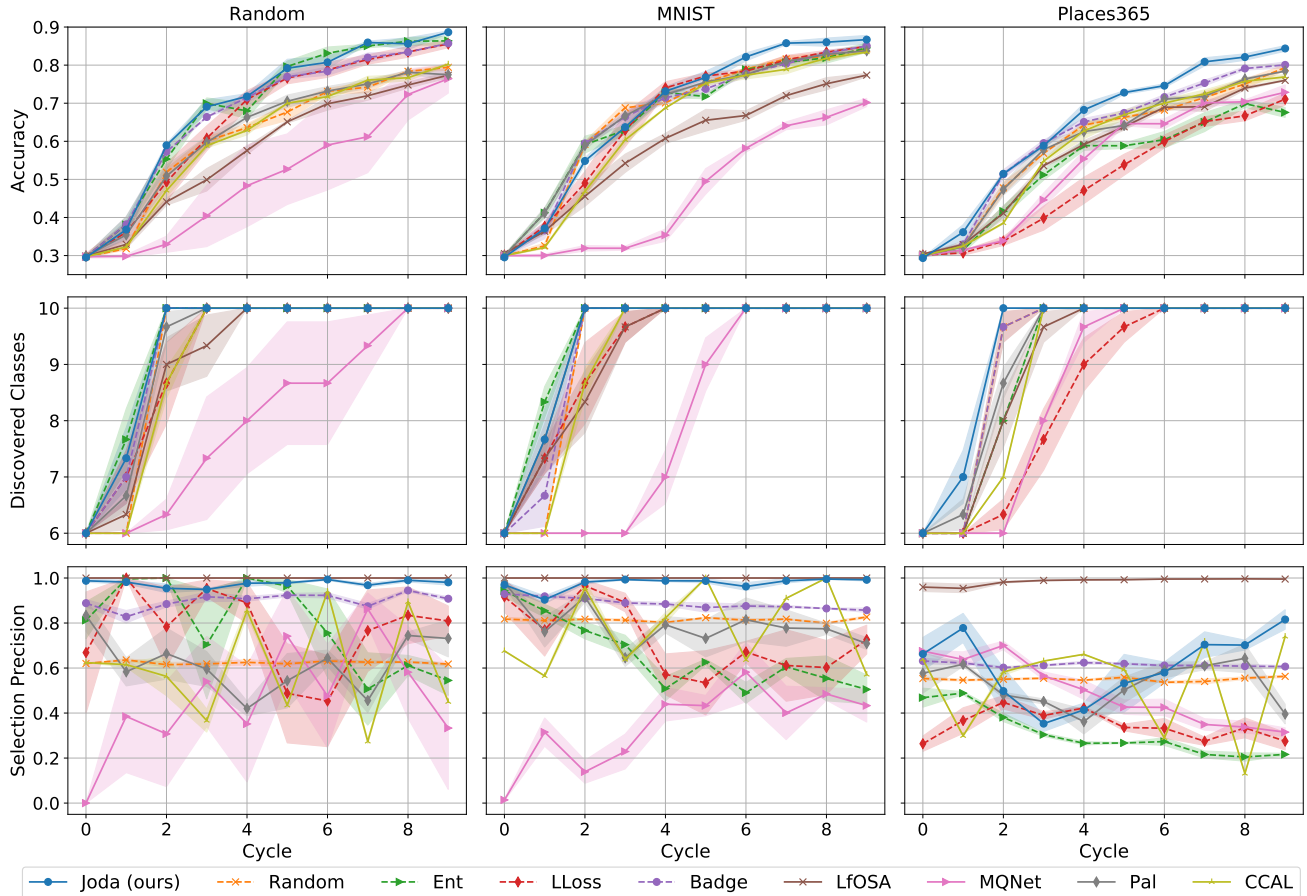


Figure 11. Comparison for CIFAR-10 with ResNet18 and indicated standard errors. From top to bottom: Accuracy, Class Detection, and Selection Precision. OOD datasets from left to right: Random, MNIST, and Places365.

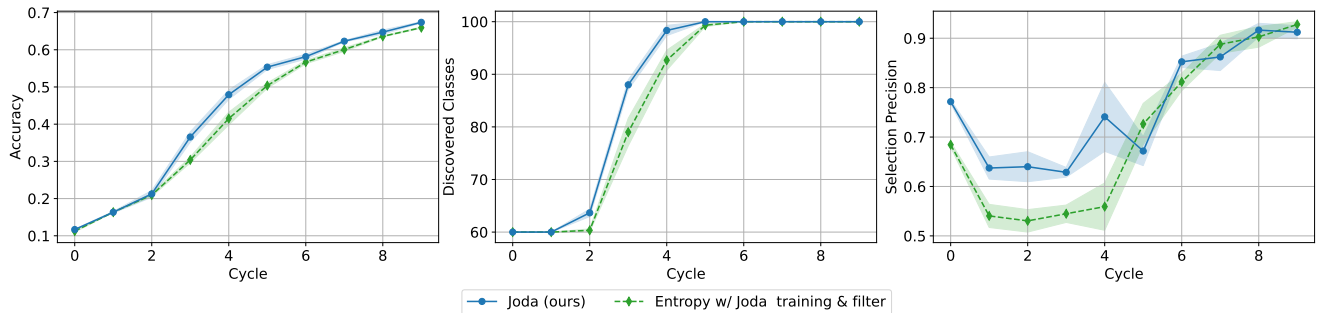


Figure 12. Comparison of different query sizes for CIFAR-100 and Places365 with indicated standard errors using ResNet18.

seen, that Joda outperforms the Entropy selection, it should be noted, that Joda’s training and filtering strategy massively improves the performance of the Entropy selection compared showcasing the effectiveness of our entangled setup.

G. Experiments on CIFAR-10

In Fig. 11, we present our results for CIFAR-10. The columns represent the OOD datasets from left to right: ran-

dom noise (Random), MNIST, and Places365. The visualizations depict the accuracy, class discovery, and selection precision from top to bottom. The classic AL methods, Ent [17] and LLoss [66], demonstrate decent performance for random noise as OOD but decrease in performance with the complexity of the OOD data and get outperformed by others for Places365. Badge [2], which incorporates diversity, achieves decent overall performance in OOD datasets. Additionally, classic AL methods pro-

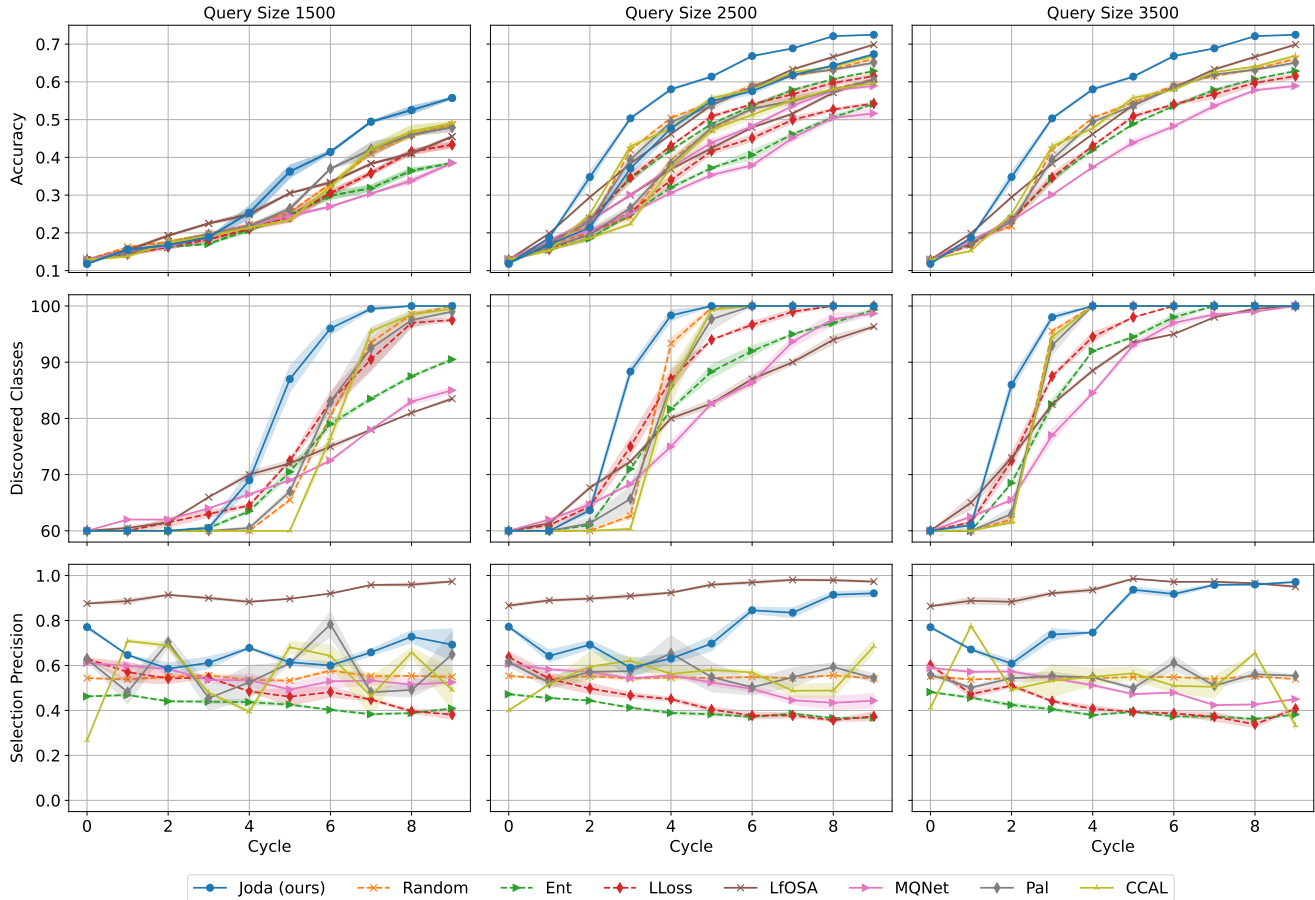


Figure 13. Comparison of different query sizes for CIFAR-100 and Places365 with indicated standard errors using ResNet18.

duce inconsistent results for precision selection. However, together with Random selection, they benefit from a small OOD ratio, as in the case of MNIST. Notably, the open-set methods based on contrastive learning CCAL [10] and MQNet [40] achieve inconsistent results. CCAL performs well for MNIST and Places365, while MQNet has difficulties with far-OOD Random and MNIST. For Places365, MQNet achieves good performance and class separation but suffers in selection precision. LfOSA [39], utilizing an additional classifier, demonstrates good precision but struggles with class discovery. However, Pal [64], CCAL, and MQNet improve their selection precision but do not surpass LfOSA or Joda in this aspect. Joda exhibits a strong performance and early class discovery with stable selection precision. For Places365, as OOD data Joda initially falls behind regarding selection precision but recovers after a few cycles. In comparison to CIFAR-100, the gap between the methods is smaller, given the reduced number of classes. Overall, Joda showed the best combination of accuracy, class discovery, and selection precision.